Natural Resources for Human Health
eISSN: 2583-1194

Original Research

Received 20 July 2026
Revised 18 Aug 2026
Accepted 04 Sep 2026

Natural Resources for Human Health 2026, Vol. 6 (21s): 428–443

KEYWORDS:
Electrical Discharge Machining; Sae 1015 Mild Steel; Taguchi Method; Anova; Grey Relational Analysis; Material Removal Rate; Surface Roughness

Multi-Objective Optimization of EDM Process Parameters in Machining SAE 1015 Mild Steel: A Taguchi-DOE Approach

Sushil Kumar Nirvan[1], Shri Krishna Mishra[2,*], S. Om Prakash[3,] K Sopiya[4], H Blessed rosemary[5], R. Suresh[6]

[1]P.G Student Department of Mechanical Engineering, Suresh Gyan Vihar University, Jaipur, Rajasthan 302017, India sushilnirvan@gmail.com
[2] Assistant Professor Department of Mechanical Engineering, Suresh Gyan Vihar University, Jaipur,Rajasthan 302017, India krishna.mishra1187@gmail.com
[3]Professor Department of Mechanical Engineering, Chettinad College of Engineering and Technology
Karur 639114, Tamil Nadu, India. Pingingprakash@gmail.com
[4]Assistant Professor, Department of Aeronautical Engineering,Nehru Institute of Engineering and Technology, Coimbatore – 641105,Tamil Nadu, India. sopiyakesavan6953@gmail.com
[5]Assistant Professor, Department of Aeronautical Engineering,Nehru Institute of Engineering and Technology, Coimbatore – 641105,Tamil Nadu, India. blessedrosemaryh@gmail.com
[6]Professor Department of Mechanical Engineering, Vel Tech High Tech Dr. Rangarajan Dr. Sakunthala Engineering College, Avadi, Chennai -600062, Tamil Nadu, India. sureshr77@gmail. com
*Corresponding author: krishna.mishra1187@gmail.com

ABSTRACT: Electrical discharge machining (EDM) can cut any electrically conductive material regardless of its hardness, but low-carbon steels such as SAE 1015 have seldom been examined in a systematic way. Here, the influence of source voltage (A), discharge current (B), pulse-on time (C) and pulse-off time (D) on material removal rate (MRR) and surface roughness (Ra) is investigated for die-sinking EDM of SAE 1015 mild steel with a graphite electrode. Experiments followed a nine-run Taguchi-based plan, and the data were processed in Minitab 17 through signal-to-noise (S/N) ratios, analysis of variance (ANOVA) and linear regression. Discharge current emerged as the dominant factor for both responses. For surface roughness it was the only statistically significant factor ($p = 0.017$; 39.7% of total variation). The regression model returned $R^2 = 89.9\%$ and adjusted $R^2 = 79.9\%$, yet its leave-one-out predicted R^2 was negative, so the model should be read as descriptive and not predictive. The best S/N settings for MRR (A2B3C2D2) and for roughness (A1B1C1D3) disagree, which is why a grey relational multi-objective analysis was applied. The response optimizer put the maximum predicted MRR at 58.68 mm^3/min for 200 V, 48 A, 6.4 µs and 12.8 µs.

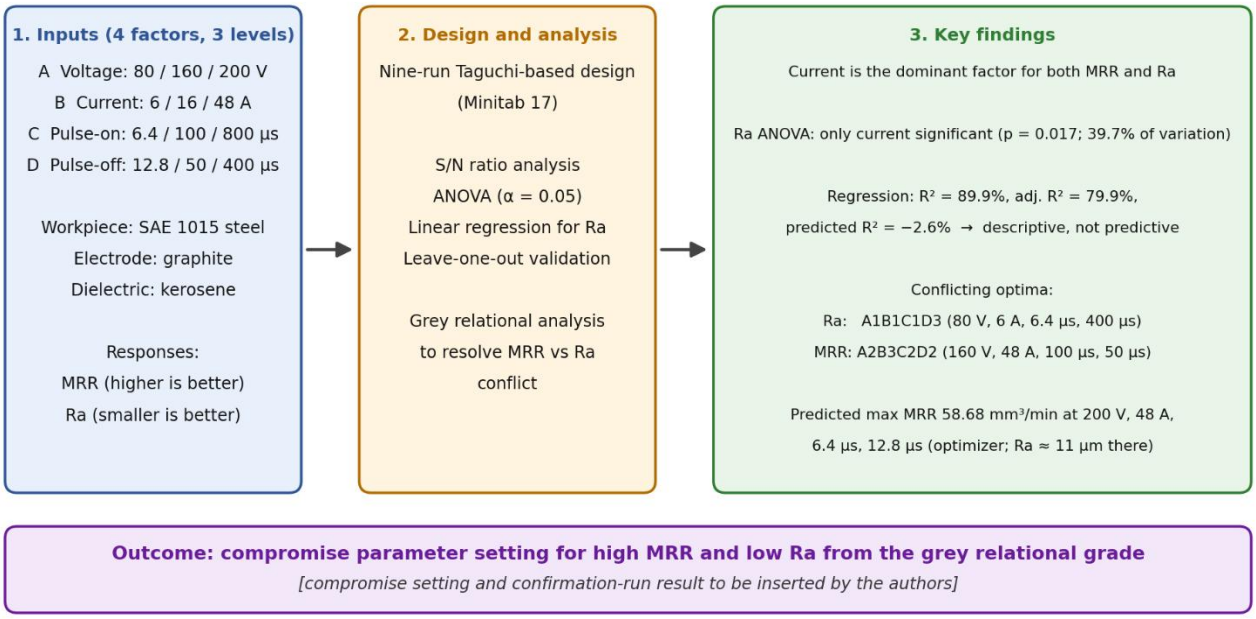
Highlights

- A nine-run Taguchi-based design was used to study four EDM parameters for SAE 1015 mild steel.
- Current dominated the response of both MRR and Ra.

Natural Resources for Human Health
eISSN: 2583-1194

- In the ANOVA for Ra, only discharge current reached significance ($p = 0.017$).
- The regression model (adjusted $R^2 = 79.9\%$) failed leave-one-out validation and is treated as descriptive only.
- MRR-optimal and Ra-optimal settings conflict; a grey relational grade is used to resolve the trade-off.

Graphical abstract



ABBREVIATIONS AND NOMENCLATURE

Symbol / abbreviation	Description
EDM	Electrical discharge machining
DOE	Design of experiments
MRR	Material removal rate (mm^3/min)
SR, Ra	Surface roughness; arithmetic average roughness (µm)
TWR, EWR	Tool wear rate; electrode wear rate
ANOVA	Analysis of variance
S/N	Signal-to-noise ratio (dB)
HB, SB	Higher-is-better; smaller-is-better
OA	Orthogonal array
GRA, GRC, GRG	Grey relational analysis; grey relational coefficient; grey relational grade
PRESS	Predicted residual error sum of squares (leave-one-out)

Symbol / abbreviation	Description
RSM, ANN, GA, TOPSIS, MCDM	Response surface methodology; artificial neural network; genetic algorithm; technique for order preference by similarity to ideal solution; multi-criteria decision making
A (V)	Source voltage (V)
B (I)	Discharge current (A)
C (T_{on})	Pulse-on time (µs)
D (T_{off})	Pulse-off time (µs)
τ	Duty cycle = $T_{on}/(T_{on}+T_{off})$
W_i, W_f	Initial and final workpiece mass (g)
t	Machining time per run (min)
ϱ	Workpiece density (g/cm^3)
ξ, γ, ζ	Grey relational coefficient, grey relational grade, distinguishing coefficient

1. INTRODUCTION

EDM erodes material by means of repeated, controlled electrical discharges that pass between a tool electrode and a conductive workpiece submerged in dielectric fluid. The tool never touches the workpiece, so the process can generate complex profiles, sharp inner corners, deep cavities and close tolerances in metals that resist conventional cutting, including tool steels, nickel-base superalloys, carbides and advanced composites. These strengths explain its broad use in the aerospace, automotive, die-and-mould and medical-device sectors.

During machining the tool and workpiece are held apart by a narrow gap filled with dielectric, kerosene in this work. A spark is initiated once the gap voltage surpasses the breakdown strength of the dielectric. The resulting local heating is enough to melt and vaporise a tiny portion of the workpiece, and the circulating dielectric then carries the debris away. Because the outcome is governed largely by the pulse parameters, they must be chosen carefully if a high MRR is to be combined with an acceptable surface finish.

A large body of work has applied Taguchi methods, RSM, GRA, TOPSIS, neural networks and evolutionary algorithms to the optimization of EDM process parameters. In wire-cut EDM, Kumar et al. [1] tuned the parameters by grey-based response surface methodology, Sharma et al. [2] used the Taguchi technique on EN-31 steel, Marelli et al. [3] surveyed optimization studies on superalloys, Tiwari and Saif [4] applied Taguchi's approach to maximise MRR on aluminium alloy 6061, and Subramanian et al. [5] treated Al/SiO_2 composites with the Taguchi method. Among die-sinking studies, Purohit et al. [6] employed GRA for M2 tool steel, while Selvarajan et al. [7] relied on Taguchi-based GRA to improve the form and orientation tolerances of a Si_3N_4–TiN ceramic composite. Mandaloi et al. [8] evaluated how a tungsten–thorium electrode influences MRR, EWR and surface finish on AISI M2 steel. Multi-response optimization was carried out with fuzzy TOPSIS by Dewangan et al. [9] and with TOPSIS by Bhuyan et al. [10]. Das et al. [11] coupled the Taguchi method with GRA for EN 31 steel; a confirmation test supported the optimum, and current was the significant factor.

Later studies have shifted toward multi-criteria decision making and data-driven models. A review by Pendokhare et al. [12] covered over 130 Scopus-indexed papers from 2013–2022 and found that the Taguchi L9 array, medium- and high-carbon steels, peak current with pulse-on time, and GRA were, respectively, the design, work materials, input variables and MCDM tool used most often. Qasem and Alsakarneh [13] demonstrated that machine-learning models can predict EDM MRR and surface roughness over several materials, with Gaussian process regression giving the best accuracy.

Several gaps remain in the literature reviewed here. (i) Most EDM optimization work targets tool steels, superalloys and composites; low-carbon steels like SAE 1015, which are common in dies, fixtures and prototypes, are seldom used as the EDM workpiece. (ii) Many Taguchi studies give only single-response optima even though MRR and Ra pull in opposite directions and their best settings usually differ. (iii) Regression models are often presented without adjusted R^2, predicted R^2 or any independent validation, which leaves their predictive value uncertain. (iv) Experimental details and repeatability are frequently too sparse for the results to be reproduced. For SAE 1015 steel, the present work responds to these gaps by (a) analysing MRR and Ra through S/N ratios and ANOVA, (b) reporting regression diagnostics, including leave-one-out validation, (c) settling the MRR–Ra conflict with a grey relational multi-objective analysis, and (d) recording the experimental conditions.

Accordingly, this study aims to: (1) quantify how source voltage, discharge current, pulse-on time and pulse-off time affect MRR and Ra; (2) rank the factors statistically; (3) build and validate a regression model for Ra; and (4) find a compromise parameter setting that gives high MRR and low Ra together.

2. IMPORTANT PARAMETERS IN EDM

Pulse-on time (T_{on}) is how long current flows in each cycle and determines the energy delivered per spark. Pulse-off time (T_{off}) is the pause between sparks, in which the dielectric de-ionises and debris is flushed out. Duty cycle is defined as $\tau = T_{on}/(T_{on} + T_{off})$. Peak current ($I_p$) is the highest current reached during a pulse and sets the discharge energy. Gap voltage (V) is the potential difference across the electrode gap, whereas electrode diameter (D) fixes the geometry of the machined feature. Overcut is the difference between cavity size and electrode size. Polarity, flushing, tool-lift time and electrode material further influence efficiency and surface integrity.

Performance is judged by MRR, surface roughness, TWR and surface integrity. MRR, the volume removed per unit time, reflects productivity. Roughness affects the service life and fatigue strength of the machined surface, and surface integrity includes the recast layer, micro-cracks, residual stresses and metallurgical changes. MRR and Ra are the responses considered in this study.

Discharges take place in the dielectric between tool and workpiece once a DC supply imposes a potential difference across the gap. Reversing the polarity changes machining performance. With straight polarity the workpiece is attached to the positive terminal, since about two-thirds of the heat is generated at the anode, which promotes a higher MRR.

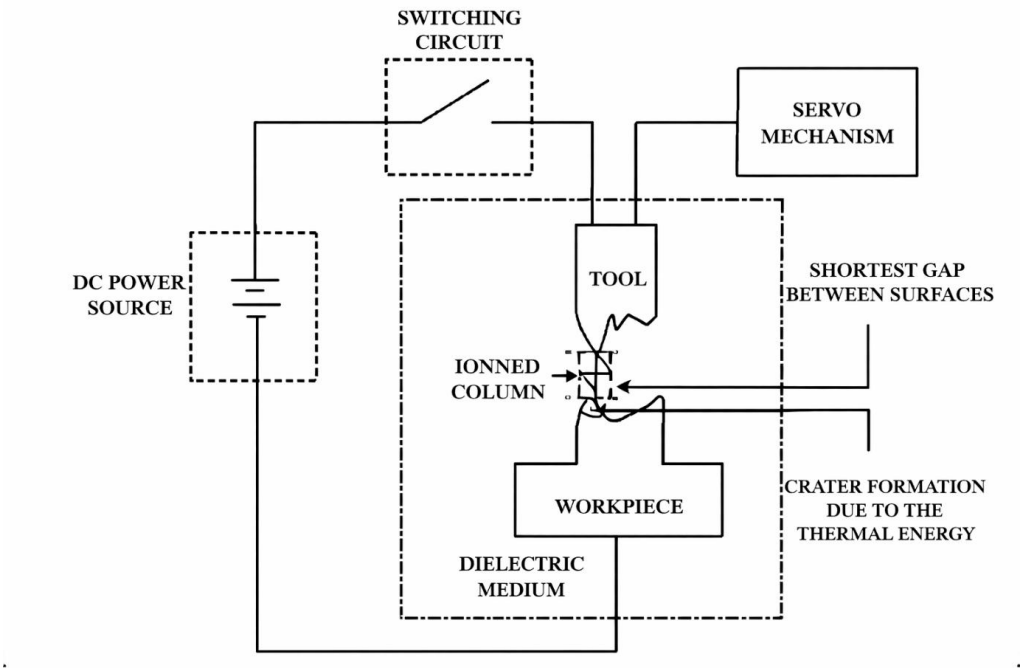


Figure 1: Basic EDM circuit and the mechanism of material removal.

Figure 1 shows the working principle. A DC source and a switching circuit produce controlled sparks across the gap; an ionised channel forms and material is removed by thermal cratering.

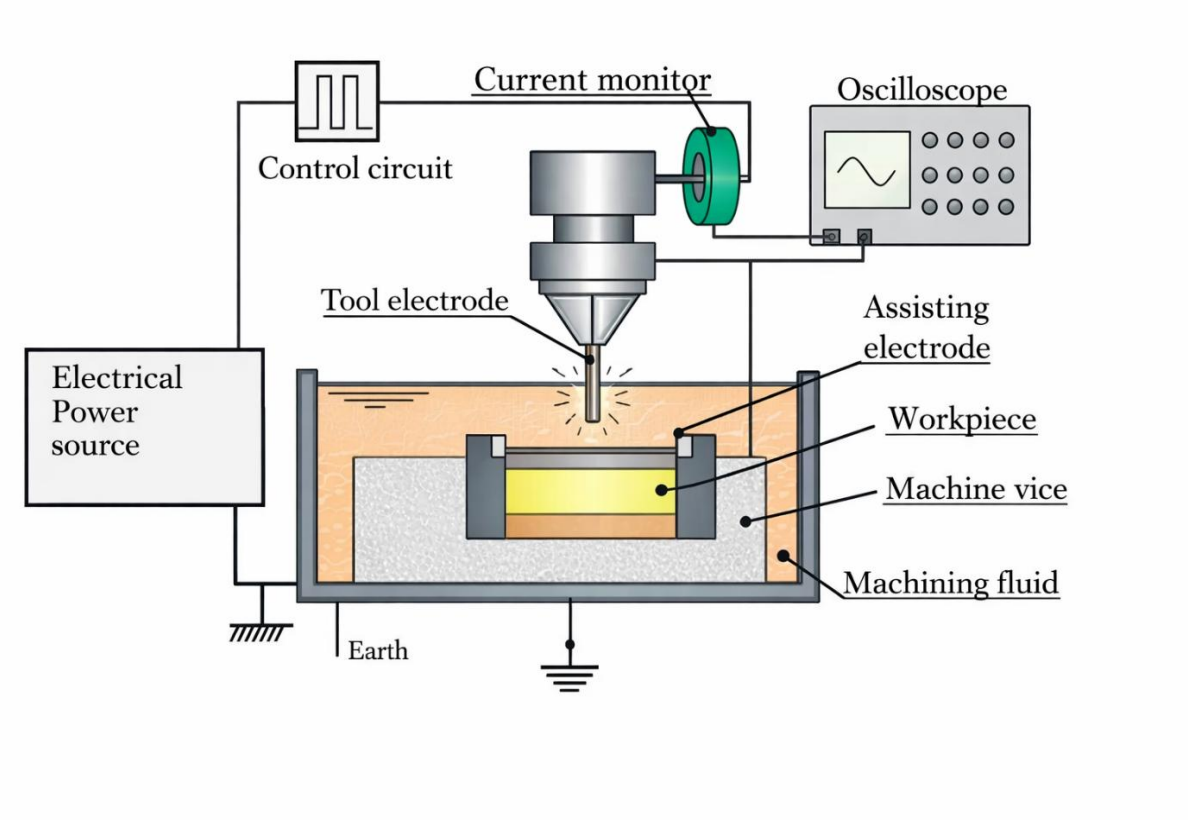


Figure 2: EDM experimental setup (schematic).

The EDM system and its monitoring and control units are shown in Figure 2. A controller sets the pulse-on and pulse-off durations, a current monitor records the discharge current, and an oscilloscope displays the pulse waveform. The tool electrode stands perpendicular to the workpiece, which is clamped in a machine vice and immersed in dielectric. The dielectric electrically insulates the gap, cools it and sweeps out the eroded particles. As the gap closes to a critical distance a spark discharge occurs, locally melting and vaporising the workpiece, and the flowing dielectric removes the debris.

3. NEED FOR OPTIMIZATION IN EDM

Optimization seeks the best result attainable with a given process. In machining it lowers cost and lead time and gives less experienced operators a sound basis for choosing parameters. EDM has many interacting parameters and conflicting responses, so trial and error is impractical. Experimental-design techniques such as the Taguchi approach and RSM cut down the number of tests required. The Taguchi-based procedure followed here is outlined in Figure 3: parameter selection, experimental plan, S/N analysis, ANOVA, regression modelling and confirmation testing.

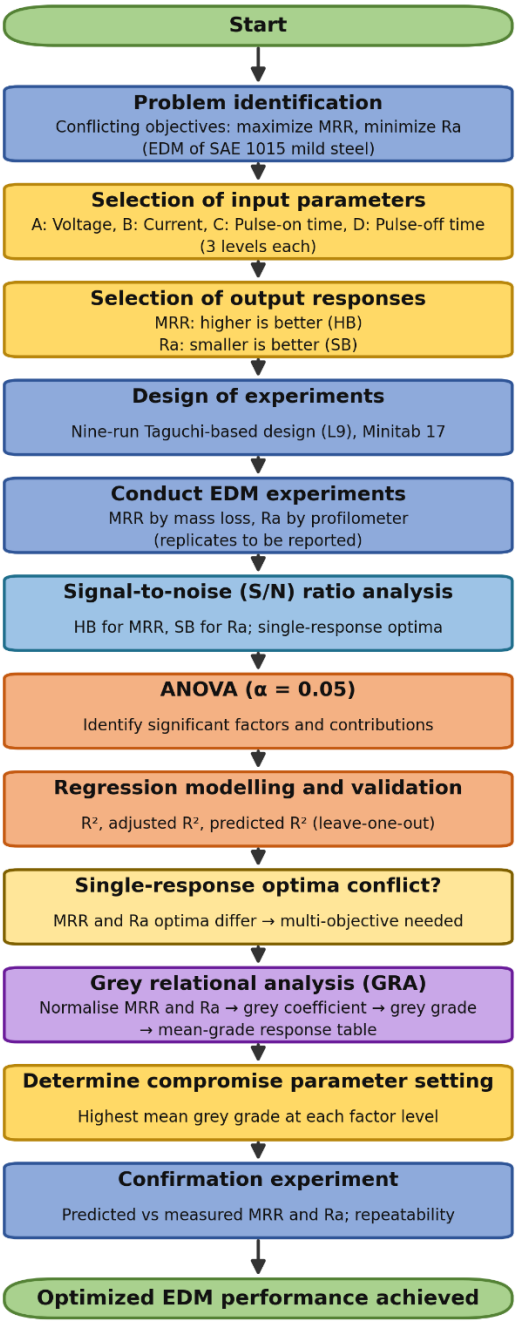


Figure 3: Taguchi-based optimization procedure for EDM.

4. EXPERIMENTAL PROCEDURE

4.1 Materials, machine and measurement

The workpiece material was SAE 1015 low-carbon steel (nominal composition 0.13–0.18% C, 0.30–0.60% Mn). Die-sinking EDM used a graphite tool electrode in kerosene, with the workpiece on the positive terminal. Other machine and specimen details are given below and need to be filled in from the laboratory records:

Natural Resources for Human Health
eISSN: 2583-1194

4.2 Parameters and levels

Four parameters were studied at three levels each (Table 1). These levels are those used in the Minitab design matrix (Table 3), the S/N response table (Table 2) and every plot, and they replace the different values (90/170/210 V, 5/15/46 A, 6.5/99/750 µs, 12.6/55/420 µs) given in the previous version of Table 1.

Table 1: Process input parameters and their levels.

Input parameter	Symbol	Level 1	Level 2	Level 3
Source voltage (V)	A	80	160	200
Discharge current (A)	B	6	16	48
Pulse-on time, T_{on} (µs)	C	6.4	100	800
Pulse-off time, T_{off} (µs)	D	12.8	50	400

4.3 Experimental design

A full factorial design with four three-level factors would require $3^4 = 81$ runs, whereas a nine-run Taguchi L9 design lowers this by roughly 89%. The L9 array has 8 degrees of freedom, exactly the $4 \times 2 = 8$ needed for the main effects; it is therefore saturated and, with categorical factors, leaves nothing for error or interactions. For that reason the ANOVA in Section 6 treats the factors as continuous variables (1 degree of freedom each), leaving 4 degrees of freedom for the residual. The resulting F and p values hold only when the response is approximately linear in each factor across the tested range.

The run matrix actually carried out (Table 3) is not a perfectly balanced L9. Factor A occurs three times at every level, but the levels of B, C and D occur 5/2/2, 3/2/4 and 4/2/3 times respectively. The level means of B, C and D are consequently partly confounded with other factors; level 2 of C (100 µs), for instance, appears only in runs 5 and 6, which also share A = 160 V and D = 12.8 µs. Conclusions about main effects need to be read with this limitation in mind.

Minitab 17 was used for the analysis. Each response was converted to an S/N ratio, using smaller-is-better for Ra and higher-is-better for MRR, and significance was assessed at $\alpha = 0.05$.

5. DATA REDUCTION

MRR was determined from the mass lost by the workpiece:

$$MRR = [(W_i - W_f) \times 1000] / (\rho \cdot t) \quad (1)$$

where W_i and W_f are the initial and final workpiece masses (g), ρ is the density (g/cm^3), t is the machining time (min), and MRR is expressed in mm^3/min. (Since 1 cm^3 = 1000 mm^3, MRR in mm^3/min cannot be equated to g/h, as was done in the previous version.)

Surface roughness was expressed as the centre-line average Ra, i.e. the mean of the absolute deviations of the profile y(x) from its mean line over the sampling length L:

$$Ra = (1/L) \int_0^L |y(x)|\, dx \quad (2)$$

The S/N ratios were calculated for n observations y_i as:

$$(S/N)_{SB} = -10 \log_{10} [\, (1/n) \Sigma\, y_i^2 \,] \quad \text{(smaller is better, Ra)} \quad (3)$$

$$(S/N)_{HB} = -10 \log_{10} [\, (1/n) \Sigma\, (1/y_i^2) \,] \quad \text{(higher is better, MRR)} \quad (4)$$

6. RESULTS AND DISCUSSION

6.1 Effect of the parameters on MRR

Figure 4 presents the main effects of the four factors on mean MRR. MRR climbs as voltage goes from 80 V to 160 V and drops at 200 V. It rises sharply with discharge current across 6–48 A. For pulse-on time, MRR increases from 6.4 µs to 100 µs and then declines at 800 µs; for pulse-off time it increases from 12.8 µs to 50 µs and declines at 400 µs. A higher current and a longer pulse raise the discharge energy, and hence the volume melted per spark, while very long pulses and long pulse-off intervals, which lower the spark frequency, probably reduce the net removal rate. These mechanisms are suggested as plausible explanations and were not tested separately.



Figure 4: Main effects of the factors on mean MRR.

The main effects plot of the S/N ratios (higher is better) for MRR is given in Figure 5. The S/N ratio peaks at 160 V (A2), 48 A (B3), 100 µs (C2) and 50 µs (D2), so A2B3C2D2 is the combination favourable to MRR.

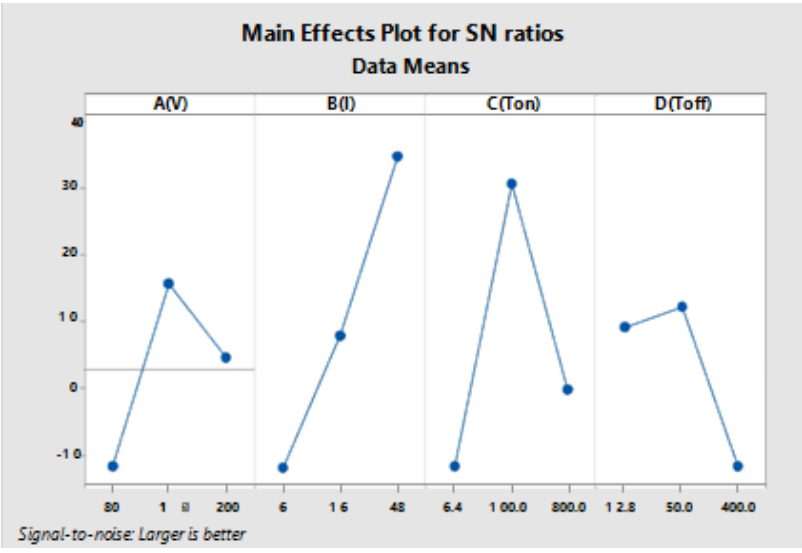


Figure 5: S/N-ratio main effects for MRR (higher is better).

Figure 6 gives the relative influence of each factor on MRR as its share of the total of the four S/N ranges (delta values). Current accounts for the largest share (33.33%), followed by pulse-on time (about 30%), voltage (19.53%) and pulse-off time

(16.97%). This is a ranking from the S/N response table, not an ANOVA percentage contribution. The earlier statement that "factor B is pulse-on time" was an error: B is the discharge current and C is the pulse-on time.

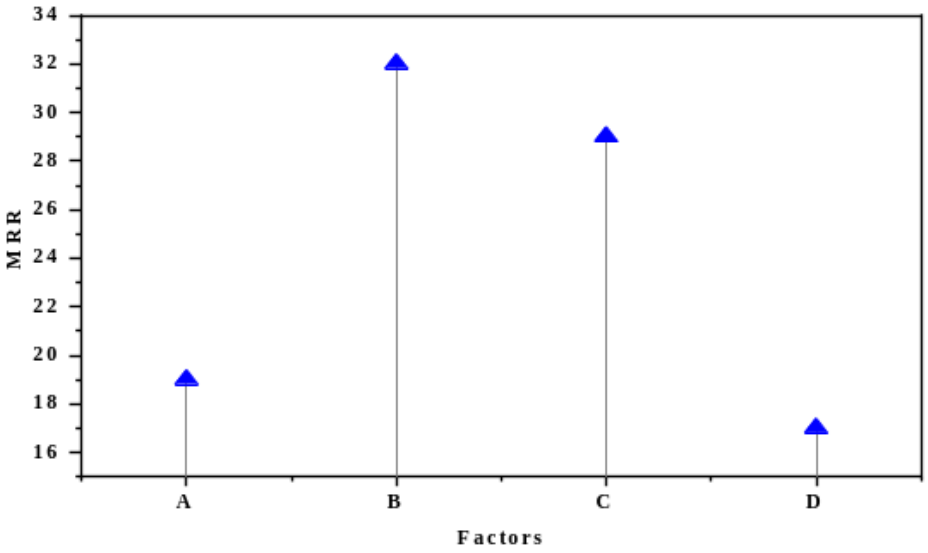


Figure 6: Relative influence of each factor on MRR (share of S/N range).

The MRR data for the nine runs, the MRR S/N response table and the MRR ANOVA table are missing from the manuscript and have to be added (the MRR column appears in Table 8). The earlier statement that "all p-values are above 5%, so interaction effects do not contribute" is invalid, because p-values test main effects and no interaction was modelled. If every main-effect p-value exceeds 0.05, the right conclusion is that no factor was statistically significant at $\alpha = 0.05$ with 4 residual degrees of freedom, which does not imply that the factors have no effect.

6.2 Effect of the parameters on surface roughness

The S/N response table for Ra (smaller is better) is in Table 2 and the experimental data are in Table 3. A larger S/N value means lower roughness, so the best levels are 80 V (A1), 6 A (B1), 6.4 µs (C1) and 400 µs (D3). The S/N range is largest for current (11.69 dB, rank 1), then pulse-on time (10.80 dB), pulse-off time (6.39 dB) and voltage (6.38 dB). The effect of current is as expected, since higher current makes larger craters and a rougher surface. The apparent penalty at C = 100 µs rests on just two runs (5 and 6) that also have 160 V, 12.8 µs and a high current, so it is confounded with those factors (Section 4.3).

Table 2: Response table for S/N ratios (dB) for Ra, smaller is better.

Level	A (V)	B (I)	C (T_{on})	D (T_{off})
1	−9.070	−8.183	−8.096	−13.875
2	−15.448	−14.044	−18.891	−14.480
3	−11.732	−19.872	−11.670	−8.096
Delta	6.378	11.689	10.795	6.385
Rank	4	1	2	3

Level means were recomputed from Table 3 and agree with the Minitab output.

Table 3: Experimental plan and results for Ra with S/N ratios.

Run	A (V)	B (A)	C (µs)	D (µs)	Ra (µm)	S/N (dB)
1	80	6	6.4	400	2.62	−8.3660
2	80	6	800	12.8	2.87	−9.1576
3	80	16	6.4	400	3.05	−9.6860
4	160	6	800	12.8	2.68	−8.5627
5	160	16	100	12.8	8.32	−18.4025
6	160	48	100	12.8	9.31	−19.3790
7	200	6	6.4	400	2.05	−6.2351
8	200	6	800	50	2.69	−8.5950
9	200	48	800	50	10.43	−20.3657

6.3 ANOVA for surface roughness

The ANOVA for Ra is in Table 4. The regression as a whole is significant ($F = 8.92$, $p = 0.028$). Among the individual factors only discharge current is significant ($F = 15.74$, $p = 0.017$), contributing 39.7% of the total variation; voltage ($p = 0.727$), pulse-on time ($p = 0.258$) and pulse-off time ($p = 0.142$) are not significant at $\alpha = 0.05$. The earlier claim that voltage "has an influence on SR" based on $p = 0.727$ was incorrect. With only 4 residual degrees of freedom in the nine-run design, test power is low, so non-significant factors, pulse-off time in particular, should be described as "not shown to be significant" and not as having no effect.

Table 4: ANOVA for Ra (factors entered as continuous variables).

Source	DF	Adj SS	Adj MS	F	p	Contribution (% of total SS)
Regression	4	83.0899	20.7725	8.92	0.028	89.92
A (V)	1	0.3269	0.3269	0.14	0.727	0.35
B (I)	1	36.6463	36.6463	15.74	0.017	39.66
C (T_{on})	1	4.0427	4.0427	1.74	0.258	4.38
D (T_{off})	1	7.7592	7.7592	3.33	0.142	8.40
Error	4	9.3116	2.3279			10.08
Total	8	92.4015				100.00

The "contribution" column in the previous Table 4 (18.09, 33.16, 30.62 and 18.11%) and in Figure 7 is not an ANOVA contribution; it is each factor's share of the summed S/N ranges in Table 2 (for example 6.378/35.247 = 18.09%). Figure 7 retains it solely as a measure of relative S/N influence. The percentages in the previous text (29.13, 37.66, 2.97 and 30.22%) and in the Conclusions (33.14, 30.62 and 15.62%) agree with neither source and have been removed. The ANOVA contributions are those in Table 4: current 39.7%, pulse-off time 8.4%, pulse-on time 4.4%, voltage 0.4%, and error 10.1%.

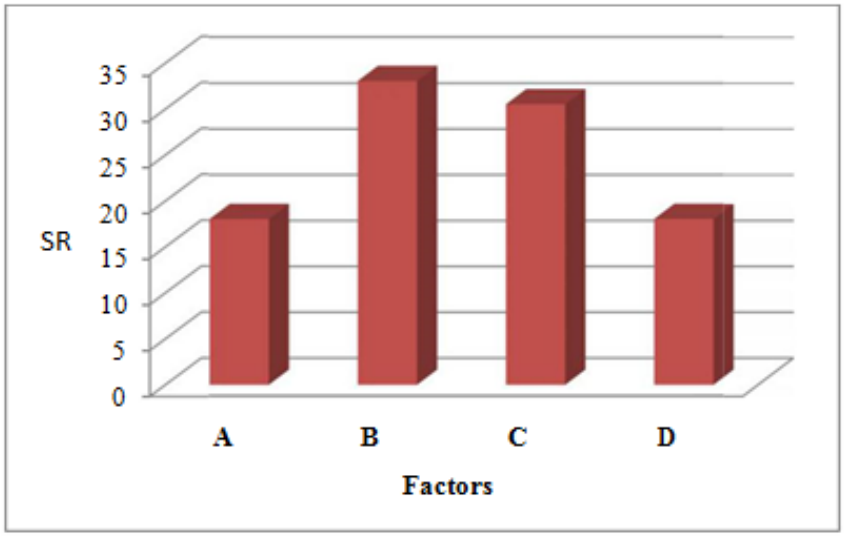


Figure 7: Relative influence of each factor on Ra (share of the S/N ranges in Table 2; not ANOVA contributions).

6.4 Regression model, diagnostics and validation

Multiple linear regression of Ra on the four parameters gave Eq. (5):

$$Ra = 3.99 + 0.0042\,A + 0.1396\,B - 0.00256\,C - 0.00795\,D \quad (5)$$

Here A is in V, B in A, and C and D in µs. Table 5 summarises model quality: R^2 = 89.92% and adjusted R^2 = 79.85% indicate that the model fits the nine observations well. The predicted R^2 from leave-one-out cross-validation (PRESS = 94.77), however, is −2.6%, meaning the model predicts a withheld run no better than the overall mean. Table 6 shows the reason: the mean absolute percentage error increases from 17.6% (fit) to 42.8% (leave-one-out), and the two high-current runs (6 and 9) are predicted especially badly when withheld. This is expected with nine runs and five estimated coefficients, because each high-current run is influential (leverage up to 0.80). Until independent runs confirm it, Eq. (5) should be treated as a descriptive trend model valid within the tested ranges and not as a predictive tool. The earlier claim of "predictive regression models with cross-validations" has been withdrawn.

Table 5: Regression model summary for Ra.

Statistic	Value
Residual standard error, S	1.526 µm
R^2	89.92%
Adjusted R^2	79.85%
Predicted R^2 (leave-one-out, PRESS = 94.77)	−2.57%
Overall F-test (4, 4 DF)	F = 8.92, p = 0.028
Largest variance inflation factor (D)	2.31 (A 1.21; B 1.34; C 2.07)
Shapiro–Wilk test on residuals	W = 0.942, p = 0.602

Table 6: Observed, fitted and leave-one-out predicted Ra (μm).

Run	Observed	Fitted	Leave-one-out prediction	Leave-one-out error
1	2.62	1.97	1.48	1.14
2	2.87	3.02	3.24	−0.37
3	3.05	3.36	3.64	−0.59
4	2.68	3.35	3.67	−0.99
5	8.32	6.54	3.64	4.68
6	9.31	11.00	14.15	−4.84
7	2.05	2.47	3.40	−1.35
8	2.69	3.22	3.62	−0.93
9	10.43	9.09	3.80	6.63

Figure 8 is the normal probability plot of the residuals. The points fall close to a straight line and the Shapiro–Wilk test ($p = 0.602$) does not reject normality, although with only nine residuals this check has little power. The interaction plot of data means is in Figure 9; since the design cannot separate interactions from main effects, it is descriptive only and no interaction term was fitted. Surface plots of Ra against current and voltage are given in Figure 10 and show Ra increasing with current at every voltage, in line with the significance of B in Table 4.

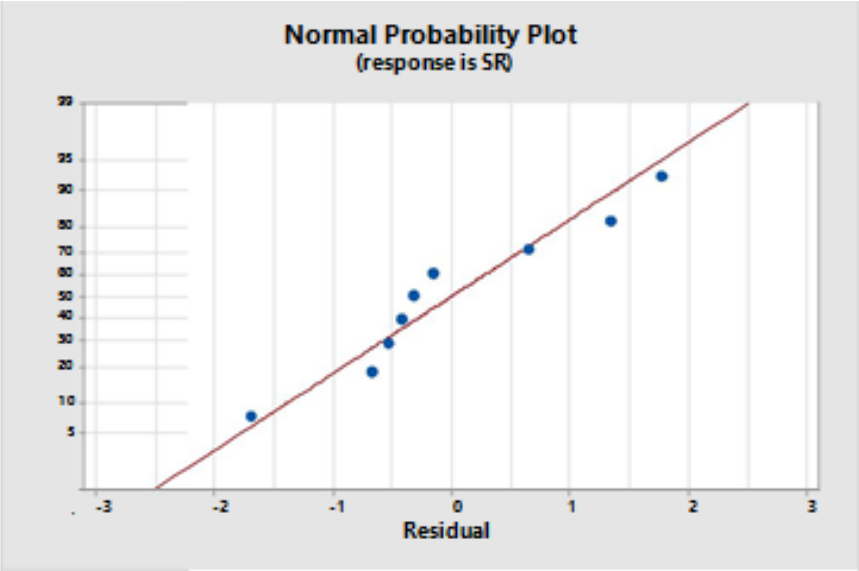


Figure 8: Residual normal probability plot for Ra.

Natural Resources for Human Health
eISSN: 2583-1194

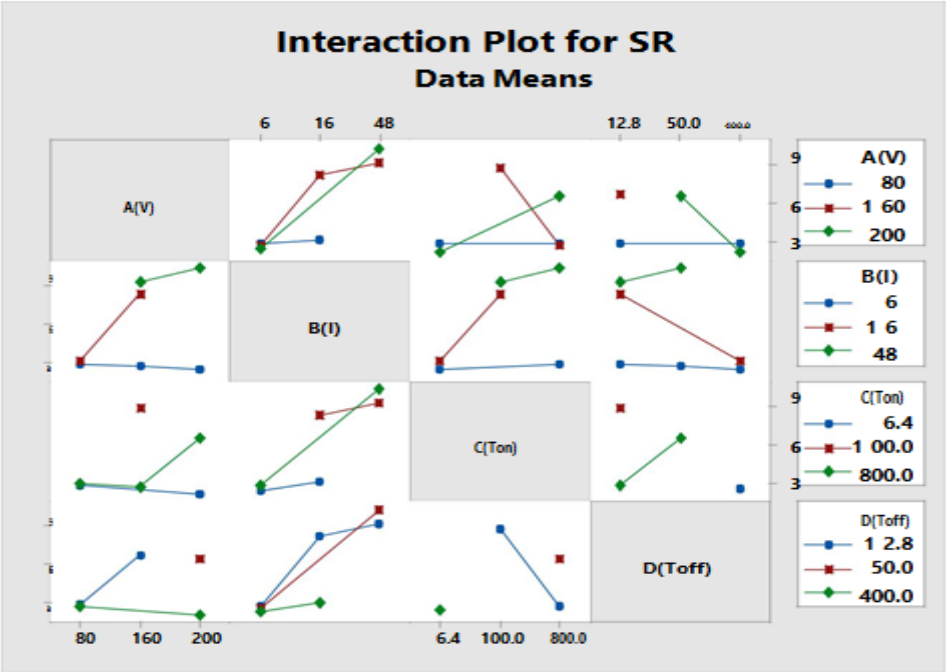


Figure 9: Ra interaction plot based on data means.

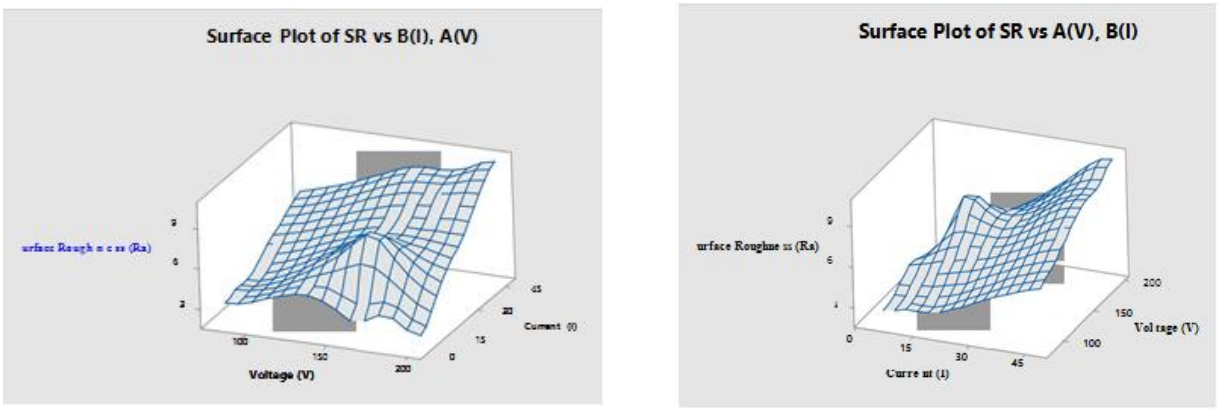


Figure 10: (a) Ra surface plot against current B and voltage A. (b) The same data with the voltage and current axes swapped.

6.5 Conflict between the single-response optima

The Taguchi S/N analysis yields different optimal settings for the two responses: A2B3C2D2 for MRR (Figure 5) and A1B1C1D3 for Ra (Table 2). The previous version claimed that A2B3C2D2 also minimised Ra, at 5.04 μm. Table 7 does not support this: the regression model of Eq. (5) predicts about 10.7 μm at A2B3C2D2, comparable to the roughest observed runs, while the best observed Ra is 2.05 μm (run 7).

Two other sets of values in the previous text (A = 134.2 V, B = 7.0 A, C = 374.8 μs, D = 200.6 μs, and a 58.67 mm^3/min "optimum" attributed to A2B3C2D2) cannot be traced to the S/N analysis and are not used. The response optimizer in Figure 11 gives a predicted MRR of 58.68 mm^3/min, but at 200 V, 48 A, 6.4 μs and 12.8 μs (the bounds of the linear model for C and D), not at A2B3C2D2. The regression model predicts Ra ≈ 11.4 μm at these settings. Because a linear model cannot reproduce the maximum in MRR with C and D seen in Figure 4, this predicted MRR should be treated with caution.

Natural Resources for Human Health
eISSN: 2583-1194

Table 7: Candidate parameter settings and predicted Ra from Eq. (5).

Setting (A, B, C, D)	Origin	Predicted Ra (µm)	MRR
A1B1C1D3 (80 V, 6 A, 6.4 µs, 400 µs)	Best S/N levels for Ra (Table 2); equals run 1	1.97 (run 1 observed: 2.62)	[insert]
Run 7 (200 V, 6 A, 6.4 µs, 400 µs)	Lowest observed Ra	2.47 (observed: 2.05)	[insert]
A2B3C2D2 (160 V, 48 A, 100 µs, 50 µs)	Best S/N levels for MRR (Figure 5)	10.71	[insert]
A3B3C1D1 (200 V, 48 A, 6.4 µs, 12.8 µs)	Response optimizer, Figure 11	11.41	58.68 (predicted)

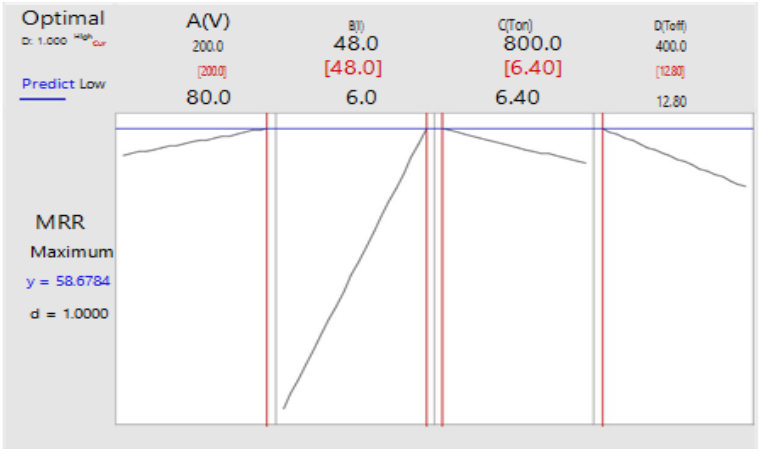


Figure 11: Response optimizer output for MRR (predicted maximum 58.68 mm^3/min).

6.6 Multi-objective optimization by grey relational analysis

Rationale for the approach. MRR and Ra are conflicting objectives (Section 6.5), so no single run or single-response optimum satisfies both and a multi-objective method is needed. GRA was chosen because (i) normalisation lets it handle responses with different units and directions, (ii) it makes no assumption about the data distribution and works with very few runs, and (iii) it is the MCDM tool most often paired with Taguchi arrays in EDM studies [11, 12]. NSGA-II or ANN-based optimization would need a validated predictive model, which is unavailable here because the predicted R^2 of the Ra model is negative (Section 6.4). TOPSIS or desirability functions are reasonable alternatives and could serve as a cross-check.

Procedure. The responses are normalised to the 0–1 range: $x^*_{MRR} = (x - x_{min})/(x_{max} - x_{min})$ for larger-is-better and $x^*_{Ra} = (x_{max} - x)/(x_{max} - x_{min})$ for smaller-is-better. The deviation is $\Delta = 1 - x^*$, and the grey relational coefficient is:

$$\xi = (\Delta_{min} + \zeta\,\Delta_{max}) / (\Delta + \zeta\,\Delta_{max}) = 0.5 / (\Delta + 0.5) \quad (6)$$

with the distinguishing coefficient $\zeta = 0.5$, $\Delta_{min} = 0$ and $\Delta_{max} = 1$. The grey relational grade is $\gamma = w_1\,\xi_{MRR} + w_2\,\xi_{Ra}$, with equal weights $w_1 = w_2 = 0.5$ as the base case. As the weights reflect engineering preference, a sensitivity check at 0.7/0.3 and 0.3/0.7 should be reported. The mean grade at each factor level is tabulated, the level with the highest mean grade is selected for each factor, and ANOVA on the grade identifies the factors that are significant for the combined objective.

Surface plots of MRR against pairs of factors are shown in Figure 12. MRR rises with current and depends on voltage, pulse-on time and pulse-off time in a curved, non-monotonic way.

Natural Resources for Human Health
eISSN: 2583-1194



Figure 12 (a, b): Surface plots of MRR against (a) current B and voltage A, and (b) voltage A and current B.

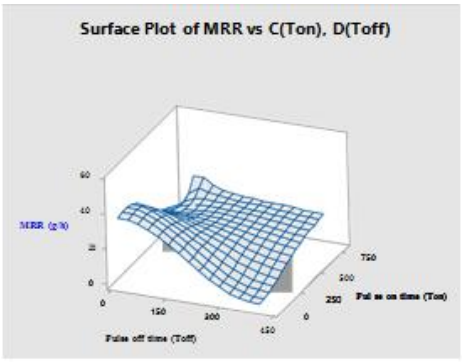


Figure 12 (c): MRR surface plot against pulse-off time D and pulse-on time C.

6.7 Confirmation experiments and comparison with the literature

A confirmation run at the compromise setting should be reported, giving the predicted and measured MRR and Ra, the percentage error between them and the repeatability of the measurements.

The previous text compared the present MRR of 58.67 mm^3/min with 54.93 mm^3/min attributed to "Yang et al." (simulated annealing), a difference of 6.37% relative to the present value. That reference is missing from the reference list, relates to a different workpiece and machine, and does not validate the present results. If kept, it should be fully cited and presented only as an indicative comparison of magnitudes.

7. CONCLUSIONS

This work examined how source voltage, discharge current, pulse-on time and pulse-off time affect MRR and Ra in die-sinking EDM of SAE 1015 mild steel, using a nine-run Taguchi-based design. The main conclusions are:

1. Discharge current is the most influential factor for both responses. It has the largest share of the S/N range for MRR (33.33%), and for Ra it is the only significant factor ($p = 0.017$), explaining 39.7% of the total variation.
2. The best S/N levels for Ra are A1B1C1D3 (80 V, 6 A, 6.4 µs, 400 µs), and the lowest observed value was 2.05 µm (200 V, 6 A, 6.4 µs, 400 µs). For MRR they are A2B3C2D2 (160 V, 48 A, 100 µs, 50 µs). Because the two optima conflict, a multi-objective approach (grey relational analysis) is required.
3. The linear regression model for Ra gives $R^2 = 89.9\%$ and adjusted $R^2 = 79.9\%$, but its leave-one-out predicted R^2 is −2.6%. It captures trends within the tested range but should not be used for prediction until confirmed by independent experiments.
4. The response optimizer gives a maximum predicted MRR of 58.68 mm^3/min at 200 V, 48 A, 6.4 µs and 12.8 µs, where Ra is predicted to be about 11 µm.

8. LIMITATIONS AND FUTURE SCOPE

- The executed run matrix is not a balanced L9 array and few residual degrees of freedom remain (4); the experiments should be repeated with a standard L9 or L18 array and replicates so that pure error can be estimated.
- Linear models cannot capture the optimum of MRR with respect to T_{on} and T_{off}; a quadratic (RSM) or machine-learning model with an independent test set should be considered, followed by evolutionary multi-objective optimization (for example NSGA-II).
- Further responses such as tool wear rate, recast-layer thickness and surface morphology (SEM) should be included, and additional workpiece materials and electrodes tested.

REFERENCES

[1] Kumar, T. Soota, and J. Kumar, "Optimisation of wire-cut EDM process parameter by Grey-based response surface methodology," J. Ind. Eng. Int., vol. 14, no. 4, pp. 821–829, Dec. 2018, doi: 10.1007/s40092-018-0264-8.

[2] S. Sharma, U. K. Vates, and A. Bansal, "Parametric optimization of EN-31 steel in wire cut electro discharge machining by Taguchi technique," Advanced Science, Engineering and Medicine, vol. 12, no. 7, pp. 881–887, Jul. 2020, doi: 10.1166/asem.2020.2645.

[3] D. Marelli, S. K. Singh, S. Nagari, and R. Subbiah, "Optimisation of machining parameters of wire-cut EDM on super alloy materials – A review," Materials Today: Proceedings, vol. 26, pp. 1021–1027, 2020, doi: 10.1016/j.matpr.2020.01.306.

[4] S. Tiwari and M. Saif, "Optimization of wire-cut EDM of aluminum alloy 6061 using Taguchi's approach for maximizing MRR," [journal name], vol. 7, pp. 2173–2181, Aug. 2020. [AUTHOR: complete the reference]

[5] K. Subramanian et al. [verify author names; the earlier list contained "PhD" artefacts], "Optimization of wire cut EDM process parameters of Al/SiO2 composites using Taguchi method," SAE Technical Paper 2020-28-0426, SAE International, Warrendale, PA, Sep. 2020, doi: 10.4271/2020-28-0426.

[6] R. Purohit, R. S. Rana, R. K. Dwivedi, D. Banoriya, and S. K. Singh, "Optimization of electric discharge machining of M2 tool steel using grey relational analysis," Materials Today: Proceedings, vol. 2, no. 4–5, pp. 3378–3387, 2015, doi: 10.1016/j.matpr.2015.07.312.

[7] L. Selvarajan, C. Sathiya Narayanan, R. Jeyapaul, and M. Manohar, "Optimization of EDM process parameters in machining Si3N4–TiN conductive ceramic composites to improve form and orientation tolerances," Measurement, vol. 92, pp. 114–129, Oct. 2016, doi: 10.1016/j.measurement.2016.05.018.

[8] G. Mandaloi, S. Singh, P. Kumar, and K. Pal, "Effect on crystalline structure of AISI M2 steel using tungsten–thorium electrode through MRR, EWR, and surface finish," Measurement, vol. 90, pp. 74–84, Aug. 2016, doi: 10.1016/j.measurement.2016.04.041.

[9] S. Dewangan, S. Gangopadhyay, and C. K. Biswas, "Study of surface integrity and dimensional accuracy in EDM using Fuzzy TOPSIS and sensitivity analysis," Measurement, vol. 63, pp. 364–376, Mar. 2015, doi: 10.1016/j.measurement.2014.11.025.

[10] R. K. Bhuyan, B. C. Routara, and A. K. Parida, "An approach for optimization the process parameter by using TOPSIS method of Al–24%SiC metal matrix composite during EDM," Materials Today: Proceedings, vol. 2, no. 4–5, pp. 3116–3124, 2015, doi: 10.1016/j.matpr.2015.07.272.

[11] M. K. Das, K. Kumar, T. K. Barman, and P. Sahoo, "Optimisation of EDM process parameters using grey-Taguchi technique," Int. J. Machining and Machinability of Materials, vol. 15, no. 3/4, 2014. [AUTHOR: add page range/DOI]

[12] D. Pendokhare, K. Kalita, S. Chakraborty, and R. Čep, "A comprehensive review of parametric optimization of electrical discharge machining processes using multi-criteria decision-making techniques," Front. Mech. Eng., vol. 10, art. 1404116, May 2024, doi: 10.3389/fmech.2024.1404116.

[13] Qasem and A. Alsakarneh, "Machine learning-based prediction of EDM material removal rate and surface roughness," J. Manuf. Mater. Process., vol. 9, no. 8, art. 274, Aug. 2025, doi: 10.3390/jmmp9080274.